International Journal of Pressure Vessels and Piping 95 (2012) 16–23

Contents lists available at SciVerse ScienceDirect

International Journal of Pressure Vessels and Piping

journal homepage: www.elsevier.com/locate/ijpvp

An insight in spatial corrosion prediction

Zahiraniza Mustaffa [a,*], Pieter van Gelder [b], Ahmad Mustafa Hashim [a]

[a] Civil Engineering Department, Universiti Teknologi PETRONAS, Bandar Seri Iskandar, 31750 Tronoh, Perak, Malaysia
[b] Department of Hydraulic Engineering, Faculty of Civil Engineering and Geosciences, Delft University of Technology, Stevinweg 1, 2628 CN Delft, The Netherlands

ARTICLE INFO

Article history:
Received 30 March 2011
Received in revised form
11 March 2012
Accepted 8 May 2012

Keywords:
Fluid–structure interactions
Vortex
External corrosions
Offshore pipelines

ABSTRACT

Recent discoveries on fluid–structure interactions between the external flows and circular cylinders placed close to the wall have added new values to the hydrodynamics of unburied offshore pipelines laid on a sea bed. The hydrodynamics of waves and/or currents introduced vortex flows surrounding the pipeline. External corrosions formed in the pipelines were assumed to be partly contributed by such fluid–structure interactions. The spatial consequences of such interactions were of interest of this study. This paper summarizes selected previous experimental and numerical works reported by literature on these discoveries. Actual field data were utilized in this study for further validation. The characteristics of corrosion orientations in the pipelines were studied comprehensively using simple statistics and results were discussed. Results adopted from the field data acknowledged well to the hypothesis from the reported literature. The updated knowledge from this fluid–structure interaction is hoped to benefit the industry and constructively incorporated into the current subsea pipeline designs.

1. Introduction

Studies on corrosions in pipelines have received numerous attention among researches not only in the past, but also in the present day. These studies were mostly related to understanding corrosion development in time, so as to predict the reliability of the structure for future operation. Knowledge on corrosion prediction in *space*, however, is still not well understood and should also be a major concern among researchers. Corrosion prediction in space can be explored in various ways but this paper attempts to gain some insights with the aid of hydrodynamics.

Recent discoveries on fluid–structure interactions between the external flows (currents and/or waves) and circular cylinder placed close to the wall have added new values to the hydrodynamics of unburied offshore pipeline placed on a sea bed. The hydrodynamics of waves and/or currents introduced vortex flows surrounding the cylinder. When a horizontal circular cylinder is near a wall, the presence of the wall changes the symmetric flow. The hydrodynamics of wave and/or current around the structure can result in the generation of sheet vortices. A vortex, as shown in Fig. 1 can be seen in a spiraling motion of water around a center of rotation. As the flow moves over the cylinder, the water deforms, rotates and because of the relatively high velocity, shears and forms a vortex. A group of vortex is called vortices (Fig. 1), and they contain a lot of energy in the circular motion of the water. These vortices are not stable and shed alternately around the cylinder.

In the context of offshore engineering, the cylinder and wall represent (unburied) pipeline and sea bed, respectively. A structure like pipeline placed in shallow waters behaves under the influence of waves and/or currents. Due to the complexity of the sea floor contours coupled with the interactions between the environmental effects like winds, tides, waves and currents and the shore area, it may be difficult to simply assume the most dominant flow that governs the area of interests. It may be wise in some cases to consider both effects.

Similar to the cylinder, the hydrodynamics of flows surrounding a pipeline will also capable to generate vortices. The unstable vortices will shed alternately around the structure. In the present work, external corrosions formed in offshore pipelines are assumed to be partly contributed by these fluid–structure interactions. The main objective of this paper is to highlight spatial consequences of corrosions from such interactions. The present work tends to validate theories from previous reported researches (experimental and numerical) on fluid–structure interactions using actual data from the field.

2. Theories on fluid–structure interactions

Earlier studies have demonstrated the significance of vortex formations surrounding a circular cylinder placed on a wall [1,2]. These studies were looking at the response under different vertical

* Corresponding author. Tel.: +60 53687296; fax: +60 53656716.
E-mail addresses: zahiraniza@petronas.com.my, mzahiraniza@yahoo.com (Z. Mustaffa).

0308-0161/$ – see front matter © 2012 Elsevier Ltd. All rights reserved.
doi:10.1016/j.ijpvp.2012.05.002

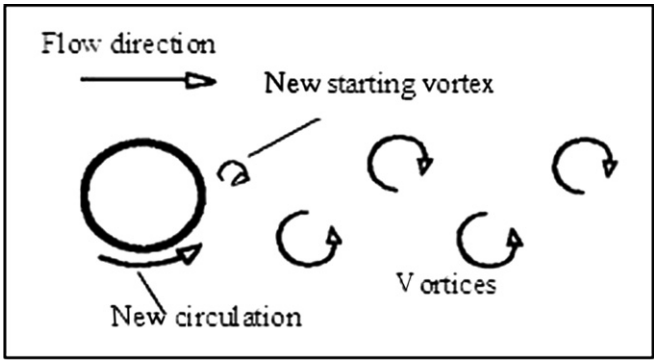

Fig. 1. Vortex formation surrounding a circular structure.

distances between the wall and the cylinder. The analysis in this paper was restricted to those very close to the wall (with vertical distance between the wall and the lower part of the cylinder very close to zero), resembling an unburied pipeline laid on the sea bed.

Numerical simulations of the wave action on a horizontal circular cylinder using the finite element method were carried out [1]. Also computed were the wave force coefficients and velocity fields and these were later verified with results reported [3]. Whereas the other studies dealt with understanding vortex characteristics exerted by cross flows around a horizontal circular cylinder [2].

For pipelines very close to the sea bed with a given ratio e/D of 0.09 (approximately 0), both the wave crest and trough produced vortex flows to the cylinder [2]. [Here e denotes the distance between the sea bed and the lower part of the pipeline and D is the pipe diameter]. They numerically predicted the streamlines at different moments in one wave period, T. From their observations, vortex would form whenever the wave crest and trough passed over the cylinder, even though these happened at different moments in a single T. The locations of these vortices, however, differed from each other, in which the one formed by the wave crest would take place at the downstream section of the cylinder while the other one developed upstream it. Once a vortex formed by the wave crest at $t/T = 0$ s as show in Fig. 2, it would undergo several phases of development accordingly: (i) increased in size and velocity (until $t/T = 0.25$ s), (ii) reduced in velocity, and partially dissipated ($t/T = 0.33$ s), (iii) non-dissipated vortex converted to the upstream, (iv) another vortex formed by wave trough at the upstream section ($t/T = 0.65$ s) and (v) vortex at the downstream section was weaker than downstream due to cancellation effect ($t/T = 0.8$ s). Due to high velocities in the vortex, the upper part of the cylinder for both upstream and downstream sections was believed to be prone to material loss.

With the aid of a particle image velocimetry probe, similar vortex formation was also visualized [2]. Since this work only involved cross flows and e/D was equal to 0, the location of the vortex was only limited to the downstream section of the cylinder and no flow passed under the cylinder, as shown in Fig. 3. This huge vortex has a diameter larger than the cylinder and comprised many small vortices. These vortices, however, were unstable and could instantly move further downstream. Nevertheless, they dissipated with time. It could be speculated then that the downstream section of the cylinder, especially the upper part prone to vortex activities. In the

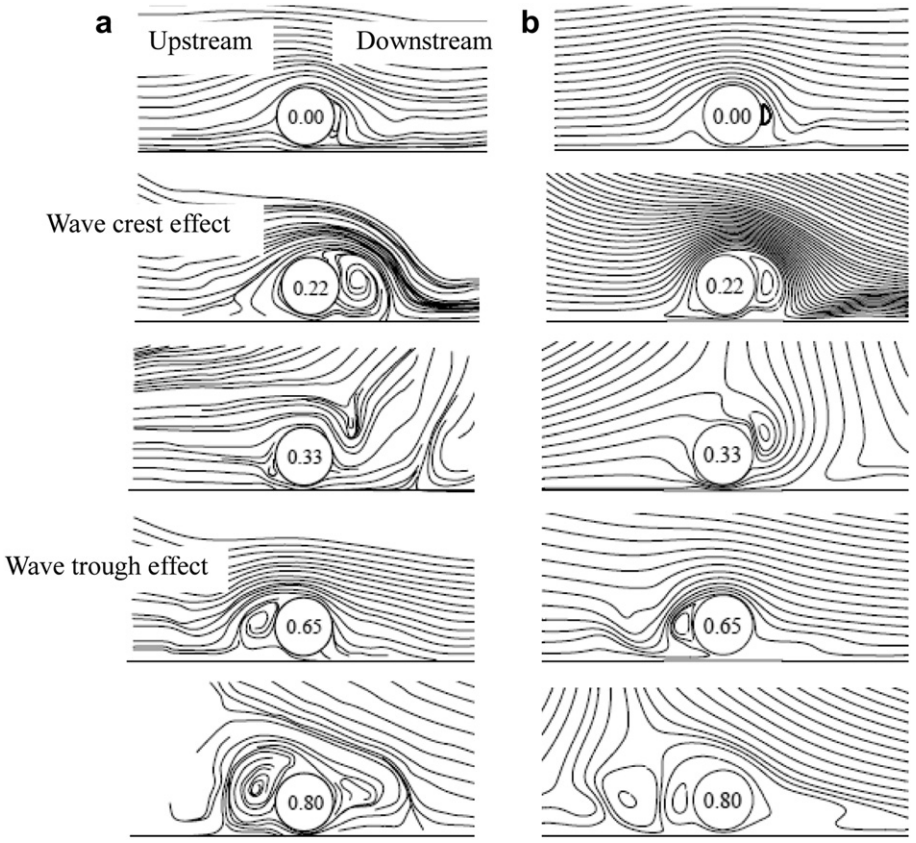

Fig. 2. Streamlines near circular cylinder at various values of t/T (shown by the number in the circle) for $e/D = 0.1$. (a) Numerical work by [1] (b) Experimental work by [3] (Adapted from [1]).

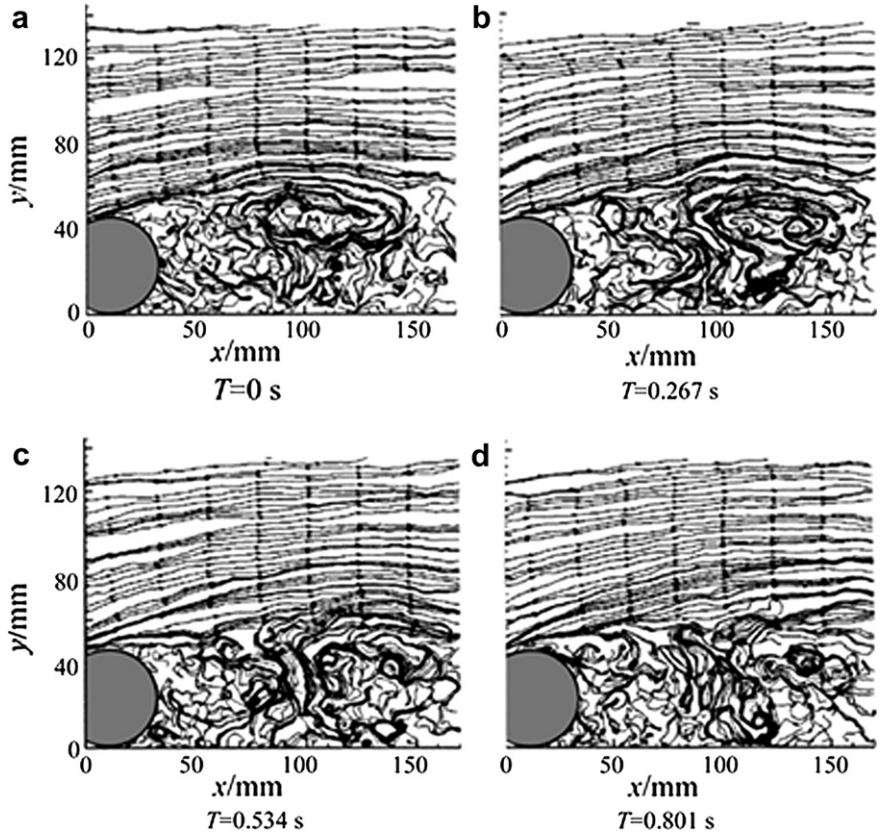

Fig. 3. Vortex at downstream section of circular cylinder at $e/D = 0$. (Here T denotes time taken by the particle image velocimetry probe to capture images, x and y are the horizontal and vertical distances measured from the cylinder, respectively) (Adapted from [2]).

case of a pipeline in particular, such vortex activities would lead to material loss i.e. corrosions would take place.

It is now understood that velocities of the flow play a significant role in the fluid–structure interactions. Previous work by [4] amply explains how water velocity influences the degree of metal loss or corrosion. The author summarized contributions to corrosion losses at different water velocities for sea water temperature of 20 °C. Even though the work was meant for early corrosion loss, it could still provide some basic ideas on the proportional impact of corrosion loss at different magnitudes of velocity. The study by [4] showed that the highest corrosion loss was observed at a high velocity of 0.45 m/s compared to other lower velocities (0.35, 0.15 m/s etc.). Indirectly, this result can be used to support the hypothesis of the present work; the high velocity exerted by the vortex is capable to erode the external surface metal of the pipeline, in which this common scenario is also known as external corrosions.

3. Validation of theories using field data

The above hypothesis was validated using actual data from the field. For this, a 28″ diameter steel offshore pipeline type API 5LX-65 containing external corrosions placed on sea bed in shallow water was chosen. Theories as proposed by [1,2] were compared with the field data. The authors' works were taken to represent as the 'models' while the pipeline candidate from the field as the 'prototype'. It is important to highlight here about similitude and scaling considerations between the models and the prototype. For simplicity purpose, the analysis was not intended to consider the similitude and scaling effects but rather focus on the prediction of the spatial consequences. The idea was to look into spatial effects of corrosions on the external surfaces of the pipeline prototype by making use of knowledge obtained from those theoretical models. Direct scaling up of the models' size or characteristics would lead to certain underestimations of the expected prototype, which was contradicted to the available information provided by the current field data.

3.1. Environmental conditions

The unburied offshore pipeline transports gas from shallow water of approximately less than 70 m to onshore. The site was at Kerteh, Terengganu, the east coast of Peninsular Malaysia, about 130 km in the South China. Fig. 4(a) shows the location of the pipeline area, circled near Kerteh while Fig. 4(b) provides an overview of pipelines layout near Kerteh shoreline. Also provided in the figure are the sea bed contours of the surrounding area.

Kerteh is a monsoon region with water temperature of 27 °C, thus experiencing a monsoonal climate created by the influences of the Southwest Monsoon in summer (Fig. 5b) and the Northeast Monsoon in winter (Fig. 5a). The latter is stronger than the former [5]. The typhoons originated from tropical waters far to the east of Peninsular Malaysia and only at rare occasions have they come close to the site [6]. Detail descriptions on the environmental conditions of the South China Sea are given in [5,6].

According to the 100-year return periods, the given current velocity, significant wave height and periods were 0.36 m/s, 5.3 m and 11.6 s, respectively. To illustrate the metocean data characteristics at the vicinity of the pipeline, hindcast data sets on wind speeds and significant wave heights at different points along the pipeline is given in Table 1. Points 1 to 5 were taken at intervals of

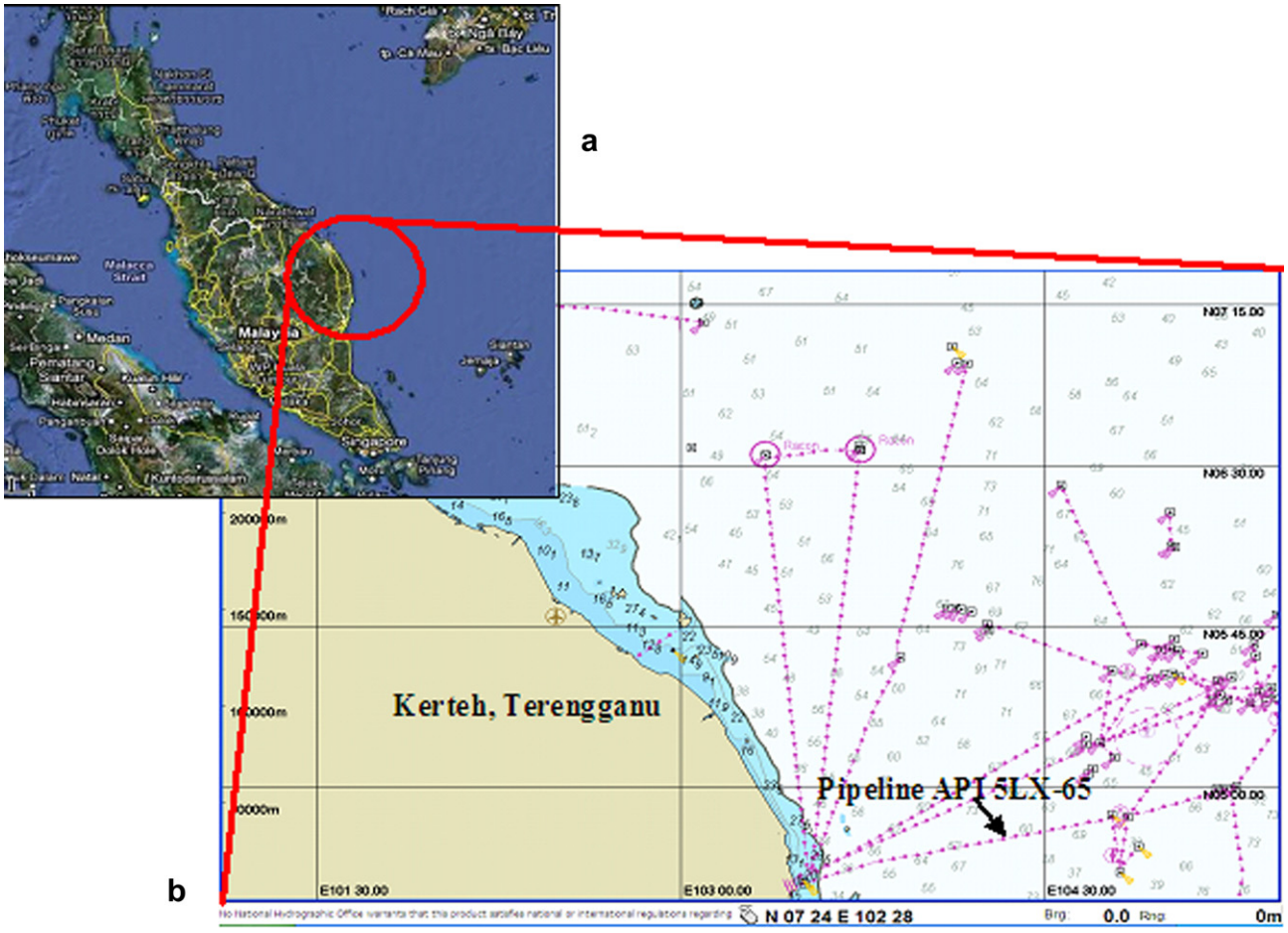

Fig. 4. Study area (a) Peninsular Malaysia (Source: Google map), and (b) shoreline of Kerteh with pipeline layouts (Source: Hydrographical map).

30 km, with Point 1 close to the shoreline while Point 5 near to the platform area. It can be seen from the table that significant wave height increases for approximately 32% from the shoreline (Point 1) towards the platform area (Point 5).

Hindcast data on current profiles (in cm/s), for which sea bottom velocities can be interpreted, are as shown in Table 2. For Points 1–5, the current velocity was simulated with respect to the vertical water depths. At each point, the magnitude of current velocity increases from the sea bed to the water surface. As water depth increases from the shore (Point 1) towards the offshore platform (Point 5), the magnitude of currents decreases. Note that all hindcast data sets were simulated for the year 2000, which is within the duration of the pipeline operational periods.

The surface current directions within the area are as provided in Fig. 5 and can reasonably applied to this particular site as surface currents are generally restricted to the upper 400 m of the ocean. As addressed earlier in [5], the dominant current direction would be in winter (Fig. 5a), acting at a cross-flow direction to the pipeline.

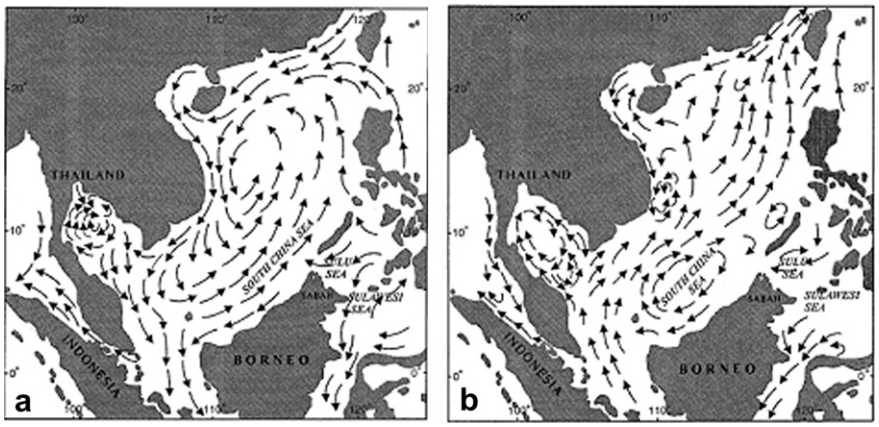

Fig. 5. Surface currents of the South China Sea in (a) winter and (b) summer (Adapted from [6]).

Table 1
Hindcast data sets on wind speeds and significant wave heights at different points along the pipeline.

	Wind speed (m/s)	Significant wave height (m)
Point 1 (103.63° E, 4.59° N)	4.07	0.65
Point 2 (103.89° E, 4.67° N)	4.56	0.75
Point 3 (104.16° E, 4.75° N)	4.83	0.81
Point 4 (104.41° E, 4.79° N)	5.00	0.84
Point 5 (104.68° E, 4.84° N)	5.13	0.86

Fig. 6 provides an enlarge overview on the distribution of attack angles of currents along the pipeline.

3.2. External interferences

Preliminary understanding of the surrounding activities in the area near the pipeline is necessary to ensure the site is free from other external interferences or threats. As reported in [7], that the area was free from anchor drags, vessel collisions and dropped objects interferences. The area was not affected by sand erosions as well. No free span exceeding the maximum allowable length was observed. Damaged caused by wave impact (splash zone) present in the pipeline but mostly taken place at the first 500 m pipeline distance as measured from the shoreline.

Marine habitats such as the mangroves and seagrass beds were not found to occupy the area but coral reefs were more likely to be found in a very shallow water ($\sim$15 m). No report was found to mention that the area has been experiencing nutrient pollution caused by the agricultural run-off or sewage pollution in coastal regions and oil pollution at offshore oil fields [7]. These effects, however, have only been investigated qualitatively and the relationship between nutrient levels and increased corrosion has not been quantified [4].

3.3. External corrosions

The pipeline was installed in 1999 and has been in operation for more than ten years. It was assumed that any defects taken place during within this period was more or less stable with the exclusion of early year defects (resulted from installation *etc.*). Emphasis was only given to external corrosion as its formation is mainly governed by the interactions between the external flows and pipelines itself.

Note that [8] divides a pipeline into two sections, namely Zone 1 and 2. The Zone 1 is the middle area that excludes 500 m upstream and downstream of the pipeline, leaving Zone 2 to cover those excluded sections. A total of 307 external corrosion defects of various types were reported by the intelligent pigging (*IP*) tool in Zone 1 with length of 128 km. It was assumed that this long pipeline has provided sufficient length to the analysis, making some predominant spatial and localized effects like marine growth and sand blasting to be reasonably ignored. Thus corrosions formation along the pipeline was only subjected to the reactions between the external flows and pipeline surface. The minimum, average and maximum wall losses were 4, 15 and 42%, respectively, calculated with respect to the actual wall thickness.

Table 2
Hindcast data sets on current velocities (in cm/s) at different points along the pipeline.

	Point 1	Point 2	Point 3	Point 4	Point 5
Near surface	9.37	43.43	38.99	27.87	21.09
30 m from surface	8.17	26.64	27.72	22.35	18.73
50 m from surface	7.54	19.89	16.65	18.62	16.19
Near sea bed	6.36	15.26	14.53	13.94	12.79

3.4. Corrosion inspection and measurement

Pigging in the maintenance of pipelines refers to the practice of using pipeline inspection gauges or *pigs* to perform various operations without stopping the flow of the product in the pipeline. The pig has to be placed in a proper *pig trap system* (Fig. 7) in order to provide a safe manner and without flow interruption. A pig is released from the upstream (*pig launcher*) and received at the downstream (*pig receiver*) of the pipeline. Pipeline pigs are inserted into and travel throughout the length of a pipeline driven by a product flow. They were originally developed to remove deposits which could obstruct or retard flow through a pipeline.

In the oil and gas pipelines, the *in line inspection* (*ILI*) tool or *smart/intelligent pigs* (*IP*) are used to provide information on the condition of a corroded pipe. The *IP* tool for instance, is able to provide corrosion defect parameters in the form of pipeline *defect depth* (d), *longitudinal length* (l) and *circumferential width* (w) as well as its *orientation* and *location*. The orientation is normally addressed as *o'clock position* with respect to pipeline cross section (illustration in Fig. 7). The present work on spatial corrosion prediction makes use of the defect parameter d as measured from the o'clock position. The magnitude of defect is given by *depth of penetration* (mm) or *amount of wall loss with respect to pipeline wall thickness* (%). The count of defects at an *IP* inspection time corresponds to its frequency of occurrence of that particular time.

4. Discussions

There are two stages involved in the spatial corrosion prediction analysis, namely the *longitudinal* and *cross section* checks. In the present work, the latter is assumed to be dependent on the former. This is because only *uniform corrosion distribution* is favorable in the longitudinal section check. Uniform distribution implies that the corrosions are developed from a mutual factor, making some predominant spatial and localized effects like marine growth and sand blasting to be reasonably ignored. Thus the corrosion formation along the pipeline was only subjected to the reactions between the external flows and pipeline surface. With the absence of uniform corrosion distribution from the longitudinal checks, results obtained from the cross section check will be less meaningful.

4.1. Longitudinal section check

Graphical presentations as shown in Figs. 8 and 9 provided examples of a longitudinal check in a pipeline. Note that distance of 0 km and 130 km referred to locations of platform (pig launcher) and Kerteh shoreline (pig receiver), respectively. Fig. 8 revealed that corrosions were developed almost uniformly throughout the longitudinal length of the pipeline. Most defects were concentrated around defect depths of 20% with some severe defects approaching 40%. Fig. 9 showed that most points along the 128 km pipeline were filled with corrosions, with no significant empty gaps observed. An average of 20 defects could be seen at every tenth km of the pipeline length with high concentration observed at the first 30 km distance (from the platform). Despite this high value, in general it could be said that there was consistent occurrence of corrosions throughout the pipeline length. The rule of having uniform corrosion distribution is now achieved. This is important to ensure the whole pipeline length was almost free from specific spatial or localized effects.

4.2. Cross section check

When uniform corrosion development was assured along the longitudinal pipeline distance, the next step of the analysis was to

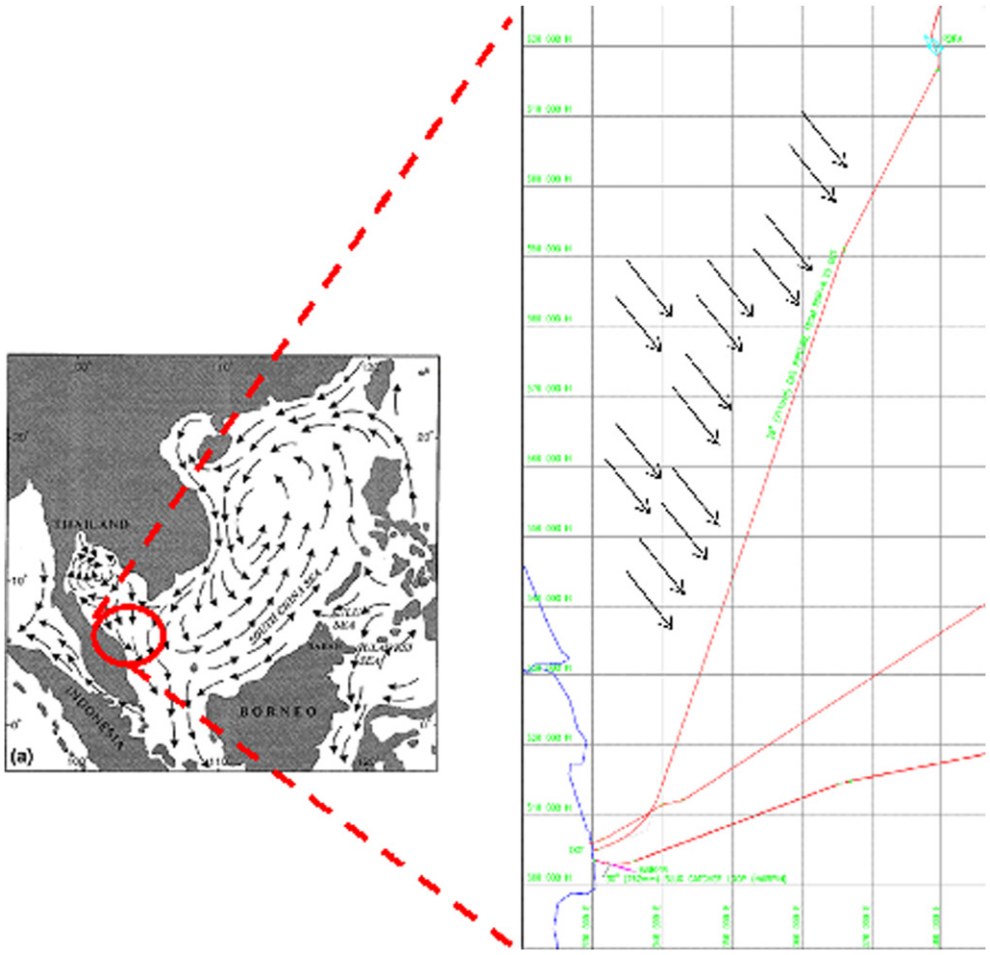

Fig. 6. Distribution of attack angles of currents along the pipeline.

understand the orientation of each defect with respect to the cross section of the pipeline, as shown in Fig. 10. Also given in the figure is an overview of clock wise orientation, as the *IP* device reports each defect with respect to its o'clock position in the pipeline.

The present work proposes spatial corrosion to be described by *regions*, as illustrated in Fig. 10. The attempt was to group *individual o'clock position* based on regions. It is important to highlight here, however, that there are various ways to define the regions and this is subjected too many arguments. In the present work, the regions were proposed based on qualitative judgment but still subjected to theories of fluids–structure interactions presented at the beginning of this section. Detailed discussion about this aspect can be referred to [11]. The pipeline was divided into three *unsymmetrical regions* (Fig. 10). Region I which was bounded from the 10 to <3 o'clock positions was proposed to conform the fluid–structure interactions mainly governed by waves. Knowing that currents prone to mostly affected the downstream sections of the pipeline, Region II was proposed and bounded from the 6 to <10 o'clock positions. The remaining o'clock positions were covered by Region III. Even though Region III was not highlighted in any reported works but it was simply adopted to cater for sea bed/soil–structure interactions.

Table 3 and Fig. 10 provide summaries of defects taken place at each region. It can be seen that Region I occupied 64% of the pipeline area followed by Region II with 24% and Region III with 11%. Details discussion on each region is given in the next section.

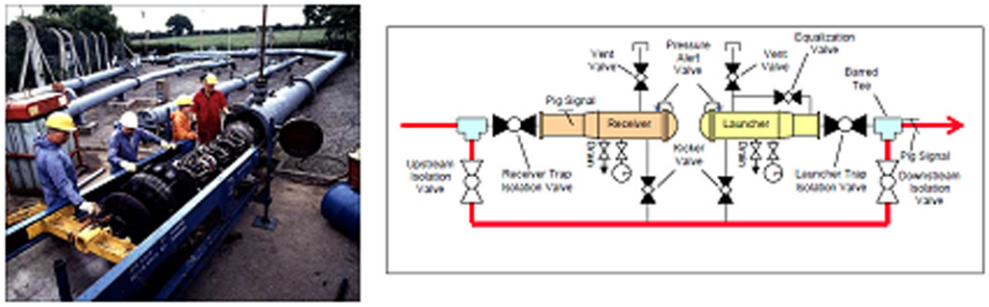

Fig. 7. Placing a pig in the pig trap system (Source: [9,10]).

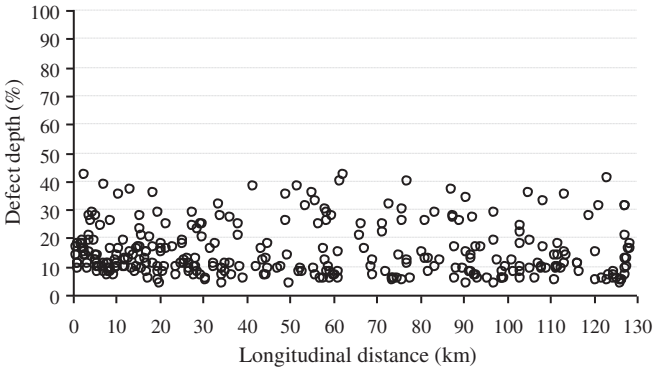

Fig. 8. Longitudinal section check in a pipeline showing defect depth (%) distributions.

5. Results interpretation

Interpreting results about external corrosions based on the proposed Region I, II and III were not something straight forward as the actual hydrodynamics that take place at the vicinity of the pipeline could be very complicated. Nevertheless, the explanation provided in this section will be entirely based on theories of hydrodynamics involving vortex characteristics.

5.1. Region I

When waves travel over the pipeline from the upstream to downstream sections, the area which covers Region I will be mostly affected by vortices. This complied well with the highest percentage of 64% obtained from Region I. Table 4 provides a summary of number of defects that occurred at certain pipeline lengths. Apparently the 11 and 12 o'clock positions contributed to the most occurrences of defects. This was indeed expected after knowing how waves travel over the pipeline. The top of the pipeline has greater tendency to be 'touched' as the waves travel over it, with the 11 and 12 o'clock positions as points which are prone to waves' activities. The first 30 km of the pipeline seemed to experience heavy corrosions compared to other remaining lengths of the pipeline. Due to the limitation of the database, it was unlikely to verify the actual underwater condition within the vicinity of the pipeline. Nevertheless, statistics allow to check for dependency between the o'clock position and longitudinal pipeline distance. The dependency check for Region I at the first 30 km was carried out using the *chi-square* (χ^2) *test* of independence. It was used to determine the presence of any significant association between the variables o'clock positions and longitudinal pipeline distance. Indirectly the method investigates whether corrosion development

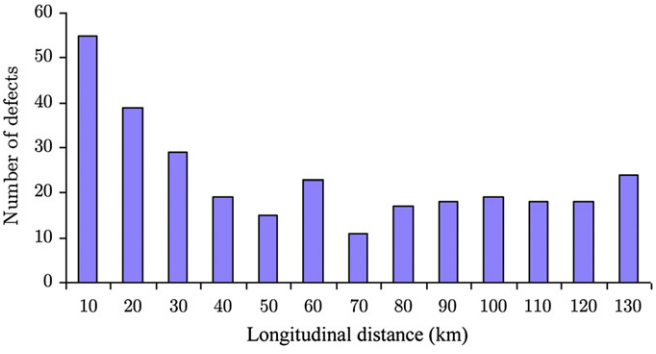

Fig. 9. Longitudinal section check in a pipeline showing number of defects.

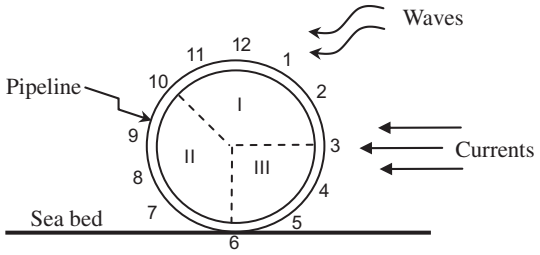

Fig. 10. Cross section view of a pipeline with details of o'clock orientation as reported by the *IP*. Also provided are the proposed regions for spatial corrosion prediction.

is depending upon its location along the pipeline. The procedures to carry out the χ^2 test could be simplified into four steps, namely (i) state the hypothesis, (ii) formulate an analysis plan, (iii) analyze sample data, and (iv) interpret results.

For the first step, two hypotheses were prepared, namely a *null hypothesis* (H_o) and *alternative hypothesis* (H_a). The former assumes that there is no association between the two variables while the latter speculates that there is an association between the two variables. Herein the hypotheses were addressed as,

H_o: O'clock position and longitudinal distance are independent
H_a: O'clock position and longitudinal distance are dependent

For the second step, the *predetermined level of significance* was assumed to be 0.05, for which the critical value ($\chi^2_{*,0.05}$) based on the *chi-square distribution table* was set to be 15.51.

To continue to the third step, it was then required to compute the degree of freedom (*DF*), the expected frequency count when o'clock position is r and longitudinal distance is c ($E_{r,c}$) and the χ^2 statistic. Based on this information, the cumulative probability value (*P*-value) could be determined. The *P*-value is the probability of observing a sample statistic as extreme as the test statistic. Equations for the above parameters are given below,

$$DF = (r-1)8(c-1) \tag{1}$$

$$E_{r,c} = (n_r{*}n_c)/n \tag{2}$$

$$\chi^2 = \sum\left[(O_{r,c} - E_{r,c})^2/E_{r,c}\right] \tag{3}$$

where r is the number of levels of o'clock positions, c is the number of levels of longitudinal distance, n_r is the number of observations from level r of o'clock positions, n_c is the number of observations from level c of longitudinal distance, n is the number of observations in the sample and $O_{r,c}$ is the observed frequency count when o'clock position is r and longitudinal distance is c.

The resulting *DF* in this analysis was computed as 8. Following this, the expected $E_{r,c}$ could also be determined. Finally, the χ^2 statistic was obtained as 34.71. (Detailed discussion about this aspect can be referred to [11]). Since the chi-square test statistic (χ_2) 34.71 exceeds the critical value ($\chi^2_{*,0.05}$) of 15.51, the null hypothesis should be rejected, thus there is a statistically significant association between o'clock position and longitudinal distance at

Table 3
Summary of defects taken place at each region.

Region	O'clock positions	Total defects
I	≥10, 11, 12, 1, 2 and <3	197
II	≥6, 7, 8, 9 and <10	74
III	≥3, 4, 5 and <6	35

Table 4
Number defects based on o'clock position in Region I.

	$0 \leq x \leq 30$ km	$30 < x \leq 60$ km	$60 < x \leq 90$ km	$90 < x \leq 128$ km
10 o'clock	8	4	6	7
11 o'clock	34	12	11	6
12 o'clock	47	4	7	7
1 o'clock	9	4	4	9
2 o'clock	10	4	2	1

Note: x is a point at any locations along the longitudinal distance of the pipeline.

the first 30 km distance of the pipeline. In other words, corrosion growth at a given o'clock position was governed by its corresponding location as measured at the longitudinal pipeline distance. This outcome implicitly concluded that some unusual corrosion activities have taken place at the first 30 km of the pipeline. Since this section of pipeline is located in shallow water zone, the wave-induced velocity could be considered to be higher. The high corrosion rate was mostly due to the amplified flow-induced shear stress experienced by the pipeline. The flow accelerates in this region and may not be directly influenced by vortices. Thus corrosions in this section would not directly have similar characteristics to those developed in other sections of the pipeline.

5.2. Region II

Region II was proposed to allow for hydrodynamics exerted by currents originated from the upstream section. Early studies speculated that the downstream section of the pipeline would experience high vortex activities [2]. Field data seemed to agree well to this hypothesis when representing this scenario onto external corrosion impacts. About 24% of the corrosions were obtained from the analysis. Being the second largest region to be affected with corrosions, this outcome could be reasonably well accepted as the pipeline was placed in a shallow water condition which allowed waves action to become the dominant environmental factor.

5.3. Region III

Region III which was assumed to be governed by the sea bed/soil–structure interactions produced the least threat to external corrosions with only 11%. Apparently vortex formation at the upstream section of the pipeline caused by the wave trough effect resulted in mild effect towards corrosion too. It was not the interest of the present work to debate much neither on soil characteristics nor soil–structure interactions because their contributions to the outcomes of this analysis were considered to be minor.

6. Conclusions

This paper is aimed at providing preliminary insights on spatial corrosion prediction using statistics approaches. The work utilized actual field data to validate earlier theoretical (experimental and numerical) works on fluid–structure interactions between external flows (waves and/or currents) and circular cylinder (pipeline) placed close to the wall (sea bed). The hydrodynamics of vortex flows produced in the fluid–structure interactions were assumed to result in external corrosions on the pipeline walls. The work critically analyzed the spatial consequences of corrosions by considering the defect orientations measured from the cross section of the pipeline. It was proposed to describe the corrosions distributions by regions, instead of analyzing it individually. Using expert judgments based on principles of the theoretical works, the region was defined by expanding the coverage of pipeline circumferential width to certain point.

Results from this analysis conformed well to both theories on waves and currents but the former was found to give higher impact to the pipeline probably because the structure was placed in a shallow water condition which was mostly governed by waves. Certain section of the pipeline experienced higher corrosion concentrations but this can be further checked using the *chi-square* (χ^2) *test* of independence.

Two new values were added to the fluid–structure interactions between waves and/or currents and pipelines in the proposed region. It was found that (i) each o'clock position (as measured with respect to pipeline cross section) would have consistent and uniform corrosions development throughout the whole pipeline length, but (ii) more corrosions should be expected for areas governed by waves, which was mainly dominated by the 11 and 12 o'clock positions.

The analyses have proven that the idea of interpreting vortex characteristics using external corrosions on pipelines could be well accepted. These preliminary insights can be further explored and the results can be used to enhance theories on hydrodynamics surrounding an unburied offshore pipeline closed to the sea bed.

Acknowledgment

The authors would like to thank Petroliam Nasional Berhad (PETRONAS), Malaysia for providing data for this project, which was financed by the Universiti Teknologi PETRONAS, Malaysia and the Schlumberger Foundation, Paris. Special thanks to Ir. Dr. Mohd Shahir Liew and Zuraida Mayeetae for their kind assistance in providing the hindcast metocean data of the study area.

References

[1] Zhao M, Cheng L, Ah H. A finite element solution of wave forces on a horizontal circular cylinder close to the sea-bed. J Hydrodynamics Ser B 2006; 18(3):139–45.
[2] Qi ER, Li GY, Li W, Wu J. Study of vortex characteristics of the flow around a horizontal circular cylinder at various gap-ratios in the cross-flow. J Hydrodynamics Ser B 2006;18(3):334–40.
[3] Jarno-Druaux A, Sakout A, Lambert E. Interference between a circular cylinder and a plane wall under waves. J Fluids Struct 1995;9:215–30.
[4] Melchers RE. Statistical characterization of pitting corrosion 1: data analysis. Corrosion (NACE) 2005;61(7):655–64.
[5] Morton B, Blackmore G. South China sea. Mar Pollut Bull 2001;42(12): 1236–63.
[6] Brink-Kjaer O, Kej A, Pushparatnam E. 1986 Environmental conditions in the South China sea offshore Malaysia: hindcast study approach, offshore technology conference, OTC 5210. p. 477–483.
[7] Nadzeri MS. 2009 Interview on pipeline candidate. Conducted by Mustaffa Z. on 25/01/2009 at PETRONAS Carigali Sdn. Bhd., Peninsular operation (PMO).
[8] Det Norske Veritas, DNV-OS-F101. Submarine pipeline systems. Oslo: DNV Standards; 2000.
[9] United Kingdom Society for Trenchless Technology. 2011 [Retrieved on 18th January 2011] (http://www.ukstt.org.uk/).
[10] PETRONAS Technical Standard. Design of pipeline pig trap system, P.T.S. 31.40.10.13; 1998.
[11] Mustaffa Z. System reliability assessment of offshore pipelines. Ph.D, Delft University of Technology, The Netherlands; 2011.